社團法人中華鋪面工程學會
Chinese Society of Pavement Engineering

ORIGINAL RESEARCH PAPER

Different AI Predictive Models for Pavement Subgrade Stiffness and Resilient Deformation of Geopolymer Cement-Treated Lateritic Soil with Ordinary Cement Addition

Kennedy C. Onyelowe[1] · Ahmed M. Ebid[2] · Frank I. Aneke[3] · Light I. Nwobia[4]

Abstract

Laboratory determination of subgrade soil stiffness (T) and modulus of resilient deformation (D) of subgrade lateritic material is a cumbersome exercise that requires sophisticated and expensive triaxial experimental set up. This, in most cases is lacking in most laboratories. The same condition is experienced during the experimentation of suction and capillary rise for the design of hydraulically bound pavement layers; the subgrade or unsaturated soils. To overcome the above costs, time and challenges, intelligent techniques; genetic programming (GP), artificial neural network (ANN) and genetic algorithm (GA) optimized polynomial linear regression (PLR) known as the evolutionary polynomial regression (EPR), have been adopted in this work to propose models for T and D under cemented and uncemented conditions of the lateritic subgrade soil treated with geopolymer cement (G). The parameters considered in this predictive model research work were capillary rise (C), suction (S), unconfined compressive strength (U) and California bearing ratio (B) as well as the varied proportions of geopolymer cement (G). At the end of the model on G-treated uncemented and cemented soil classified as A-2-6 and highly plastic soil, performance indices (SSE and R^2) were used to measure the accuracy of the models. For the uncemented case, GP and EPR showed equal accuracy with R^2 of 99.9% but with SSE of 2.9% and 2.6%, while ANN ended with 99.8% and 3.6% for the stiffness (T) prediction. For the resilient deformation (D) prediction, GP and ANN performed with R^2 of 99.3% and SSE of 6.9% and 6%, respectively, while EPR has an R^2 value of 99.2% and SSE of 6.7%. For the cemented case, EPR outclassed GP and ANN with R^2 of 99.9%; 99% and SSE 2.1%; 4.6% for the stiffness ($T^{\wedge}$) and deformation ($D^{\wedge}$) predictions, respectively. Generally, the predictive models showed consistent performance accuracy in predicting uncemented and cemented subgrade soil treated with geopolymer cement.

Keywords Pavement subgrade stiffness · Subgrade resilient deformation · Genetic programming · Evolutionary polynomial regression · Artificial neural network · Lateritic soil

✉ Kennedy C. Onyelowe
kennedychibuzor@kiu.ac.ug; konyelowe@gmail.com;
konyelowe@mouau.edu.ng

1 Department of Civil and Mechanical Engineering, Kampala International University, Kampala, Uganda

2 Department of Structural Engineering, Faculty of Engineering and Technology, Future University, New Cairo, Egypt

3 College of Agriculture, Engineering and Science Howard College Campus, University of KwaZulu-Natal, Durban 4004, Republic of South Africa

4 Department of Civil Engineering, Michael Okpara University of Agric, Umudike, Nigeria

List of Symbols

G	Geopolymer cement proportion
C	Capillary rise at 72 h curing of G-treated soil
S	Suction at 72 h curing of G-treated soil
U	UCS at 72 days curing of G-treated soil
B	CBR ratio at 24 h soaking of G-treated soil
T	Stiffness at 24 h soaking of G-treated soil
D	Modulus of resilient deformation of G-treated soil
$C^{\wedge}$	Capillary rise at 72 h curing of G-treated soil modified with OPC
$S^{\wedge}$	Suction at 72 h curing of G-treated soil modified with OPC
$U^{\wedge}$	UCS at 72 days curing of G-treated soil modified with OPC

$B^\wedge$	CBR at 24 h soaking of G-treated soil modified with OPC
$T^\wedge$	Stiffness at 24 h soaking of G-treated soil modified with OPC
$D^\wedge$	Modulus of resilient deformation of G-treated soil modified with OPC
OPC	Ordinary Portland cement
UCS (U)	Unconfined compressive strength
CBR (B)	California bearing ratio
ANN	Artificial neural network
GP	Genetic programming
EPR	Evolutionary polynomial regression
SSC	Shrink-swell cycle
SSE	Sum of squared error
R^2	Coefficient of determination
FA	Fly ash
GGBFS	Ground granulated blast furnace slag
NMC	Natural moisture content
WL	Liquid limit
WP	Plastic limit
IP	Plasticity index
MDD	Maximum dry density
OMC	Optimum moisture content
SG	Specific gravity
AASHTO	American association of state highway and transportation officials
QD	Quarry dust
SD	Standard deviation
Var	Variances
Avg	Average

1 Introduction

Pavement design and construction needs serious research attention due to complexity of the parametric consideration that is involved. Based on its response to load effects, pavement stiffness plays a critical role in reestablishing the stability of pavement systems and this was supported by Tingle and Jersey [1, 2]. Overall, the resilient deformation of geopolymer cement-treated lateritic soils are important property inputs in their mechanistic empirical pavement design for enhanced performance and resistance of the base layers and subgrade against dynamic, impulsive or critical loads [3]. Hence, the load and environmentally associated pavement response and performance are of fundamental concern to transportation geotechnical engineers [4]. Resilient deformation of pavement, its ability to absorb energy when it is deformed elastically, and tendency to release that energy upon unloading is a critical factor when assessing its service life [5]. Stabilized soils account for plastic stress accumulation for durable performance due to their safe resilient modulus [6]. It is also reported that the confining pressure,

moisture content and deviator stress levels influence the resilient and permanent deformation of treated soils [7]. For a sustainable pavement structure design and long-term pavement performance maintenance, pavement subgrade strength, a measure of its strength (the stress needed to break or rupture a material) or stiffness (the relationship between stress and strain in the elastic range) or how well a material is able to return to its original shape and size after being stressed should be perfectly analyzed, explained, described and/or predicted using certain influencing parameters such as: suction, capillary rise, California bearing ratio (CBR), stiffness, compressive strength, and modulus of resilient deformation [8–11].

Owing to the complex nature of the pavement system, pavement material characteristics, and loading conditions, there is induced complexity in analyzing and modelling the mechanism at which geopolymer cement-treated soils response. Hence, accurate prediction of optimal pavement subgrade stiffness and obtainable resilient deformation deserves evolutionary computational techniques where these non-linear interactions are perfectly traced and evaluated. Some researchers have reported the benefits of using many other soil stabilization materials and techniques in modifying pavement subgrade stiffness and hence reduction in its deformation tendencies. For example, Tang et al. [3] reported that the incorporation of geogrids at the interface between a base course layer and subgrade provides separation and minimize the degradation of the base layer caused by the mix of base aggregate and subgrade soil. They also maintained that the geogrids provide lateral restraints and prevent lateral spreading of the base aggregate, as well as increase the elastic modulus of the base layer. This report was because of the increase in the confining stresses of the interlocking and shears interaction between the geogrids and aggregate. Chen et al. [12] confirmed that the use of the geosynthetic materials had showed appreciable benefit to reducing the permanent deformation of subgrade, imposing some effect on the resilient properties of subgrade. Sahaf et al. [13] extensively discussed the benefit of accurate determination of stiffness modulus of pavement subgrade. They described important loading parameters including loading waveform, loading time, and rest time in subgrade layer. They showed that the effect of loading time could be intensified due to the increase in depth and decrease in the quality of the materials. In addition, they argued that owing to the elasto-plastic nature of subgrade material, the rest period should be considered in determination of stiffness modulus.

The use of geopolymer materials for treating soil for optimal pavement subgrade performance has proven an excellent binder that attains high strength by curing at room temperature [14]. Javdanian [15] evaluated for clayey soil specimens stabilized with fly ash and blast furnace slag based geopolymer, the unconfined compressive strength (UCS) of

improved fine-grained soils by utilizing a large database of unconfined compressive strength. Many published works have demonstrated that for geopolymer cement-treated subgrade, the super bonding between aluminosilicate and alkali solution, which produce high compressive strength, low shrinkage [16], and resistance toward acid, resistance to fire and enhance the pavement subgrade stiffness and resilient deformation characteristics.

As stochastic algorithms whose search methods model some natural phenomena, evolutionary computational techniques such as genetic programming (GP) sorts a population of computer programs genetically to resolve a problem ([17]). Whereas GP are domain-independent techniques that transmutes an assembly of computer programs into a new scheme by iteration and incorporation of genetic operations, artificial neural networks (ANNs) simulate the way the human brain analyzes and processes information via a collection of connected units or nodes called artificial neuron. An optimization of the ANN and genetic algorithm (GA), a natural selection where the fittest individuals are selected for reproduction to produce offspring or solutions of the next generation referred to as evolutionary polynomial regression (EPR) has also been largely investigated. Many researches in civil engineering have make use of the services of GP, ANN and EPR for making their predictions [14, 18–22].

The pavement subgrade stiffness and resilient deformation can be predicted using the physical properties such as liquid limit, plastic limit, plasticity index, maximum dry density, optimum moisture content, including state variables such as, degree of compaction, and stress variables like confining pressure and deviatoric stress [3]. Zhang et al. [23] proposed an optimized artificial neural network (ANN) approach based on the multi-population genetic algorithm (EPR) to effectively determine the resilient modulus of compacted subgrade soils. Coleri and Ahmet [24] reported the applicability of genetic algorithm and curve shifting methodology to the estimation of the resilient modulus at various stress states for subgrade soils using the results of triaxial resilient modulus tests. Due to the viscoelastic nature of asphalt mixes, the stiffness of these materials depends on temperature, loading time duration, rest period, and loading waveform. The interest in pavement deformations under static and dynamic loads as a measure of pavement performance and the need for a procedure whereby these deflections might be predicted in advance using reliable evolutionary prediction models such as genetic programming, artificial neural networks (ANN) and evolutionary polynomial regression (EPR) techniques fed from suitable experimental investigations of Bui Van et al. [10] has necessitated this study. Despite the numerous investigations on the application of geopolymer materials, attention has not been focused on incorporating ordinary Portland cement with the geopolymer for pavement subgrade stiffness and resilient deformation using multiple sets of soft computing techniques. The present study aims at employing GP, ANN and EPR soft computing techniques for predicting pavement subgrade stiffness and resilient deformation of geopolymer cement-treated lateritic soil with conventional cement addition using the various predictor variables: geopolymer cement proportion, capillary rise, suction, compressive strength, and California bearing ratio to predict stiffness, and modulus of resilient deformation of the geopolymer-cement treated lateritic soil. It is also important to ensure the sustainability of the entire operation; transport geotechnics and soft computing aspects of the work.

Solid waste-based ash and powder materials utilized as geomaterials or as supplementary cementing materials are generated from the combustion and/or pulverization of agro-industrial-wastes obtained from farm, household or industries. Meanwhile, sustainable materials are such that could be used by the present generation to meet their needs without affecting the ability of future generations to meet theirs [25]. Low embodied energy (EE) is used for the calcination by combustion or pulverization of these waste materials such as quarry dust (QD), rice husk (RH), sugarcane bagasse (SB), palm bunch (PB), GGBFS, fly ash (FA), etc. to generate pozzolana-based green construction materials unlike the huge EE expended for the production of conventional materials like OPC [26]. The sustainability of the waste-based construction materials depends on the advantages derived from converting waste to useful supplementary cementing materials (SCM) as well as the use of lower EE for the process. In other words, using activated waste-based ash or powder for the treatment of expansive pavement subgrade in place of the conventional building materials is very sustainable. Conversely, in the sustainability of materials and system, the cost is a vital parameter to consider. Experimental procedures in Civil Engineering could be time, energy and resource consuming [27] and so, there is a need to develop good predictive and intelligent models capable of forecasting the performance of waste-based cementing materials. Some of the predictive models that have been used to design and analyze the performance of construction materials include ANN [21] and Support vector machine [20, 28], genetic programming (GP [21]), etc. The utilization of waste-based materials, which are unconventional construction materials, has the challenge of an inexact understanding of the material properties and behaviors. These inexactitudes are due to the use of conventional materials procedures for the determination of their materials' properties [28]. Application of different machine learning-based predictive models such as SVM, GP, ANN and EPR techniquesto study the performance of these unconventional materials for building and road subgrade construction is vital to reduce the challenges of conducting repeated experiments to obtain the properties of materials. These developed models are sustainable because they save

Fig. 1 Amaba location map of soil sample
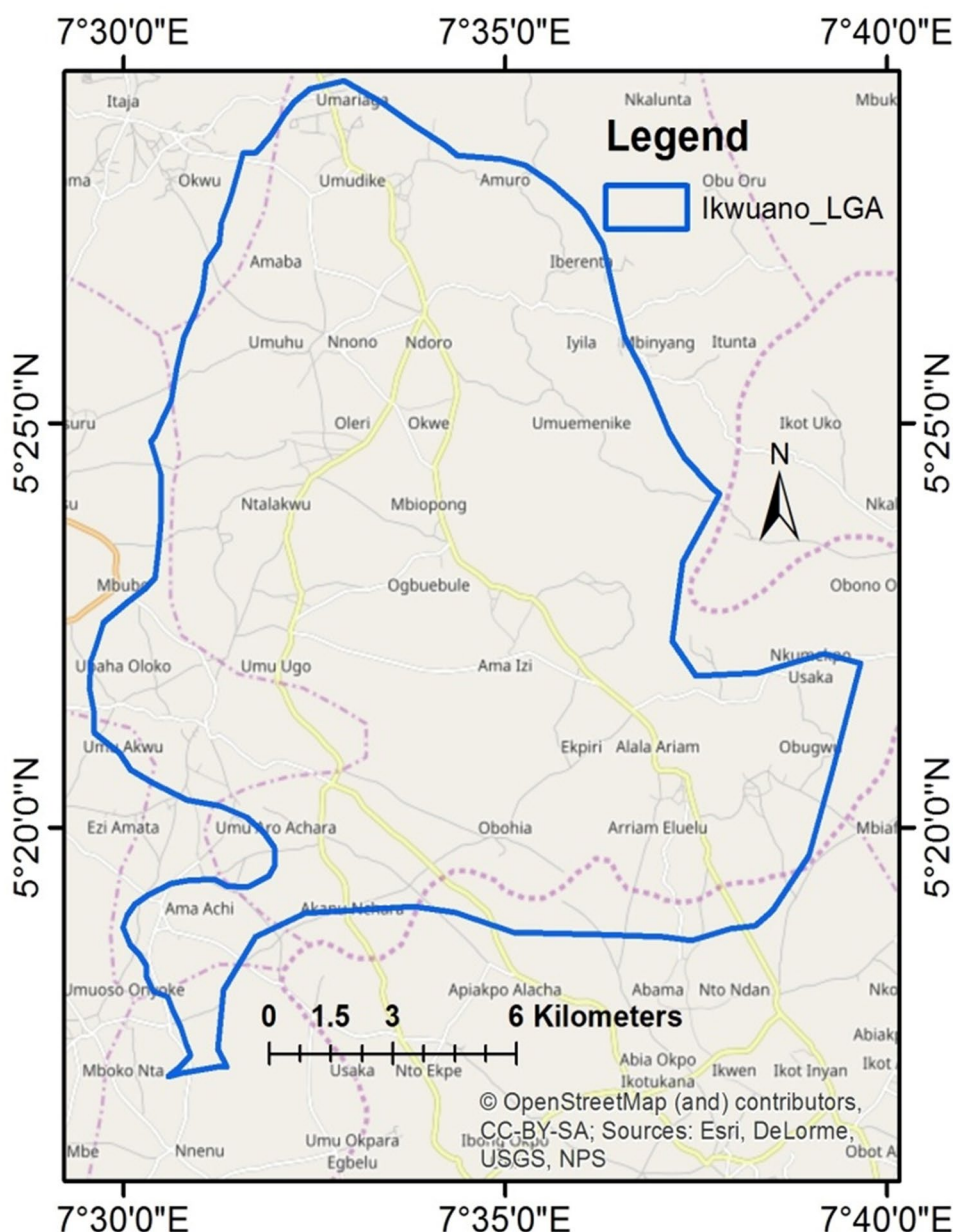
time, energy and resources that would have been used for recurrent experimental procedures aimed at obtaining the performance of green construction materials. Generally, the present work tries to use intelligent models to predict the behavior of waste-based materials-treated lateritic soil for use for the construction of sustainable pavement subgrades.

2 Materials and Methods

2.1 Materials Preparation

Figure 1 shows the map location at Amaba from where the soil sample was collected, sundried for 5 days,

rubber-pestle-mashed to remove lumps, sieved through 6.35 mm aperture sieve and stored in bags for use. The above was done in line with the requirements of BS1377-2 [29]. The quarry dust (QD), fly ash (FA) and ground granulated blast furnace slag (GGBFS) or metallurgical slag (MS) were collected as solid waste materials and prepared for use [10]. The activator needed for the formulation of geopolymer cement (GPC) was generated with NaOH in aqueous solution with mole concentration of 11 M (for eco-friendly handling) and $NaSiO_2$ mixed in the ratio of 1:1 according to the GPC design requirements of Davidovits [30] and utilized in the work of Bui Van et al. [10]. 5% of the activator solution was mixed with 50% of QD, 25% of FA and 20% of GGBFS by weight to formulate the quarry dust based

geopolymer cement (QD-GPC) designated as G in this work for the purpose of clarity. G-treated uncemented soil was achieved by deeply mixing the predetermined proportions of the formulated geopolymer cement with the soil while G-treated cemented soil was achieved by deeply mixing the predetermined proportions of the formulated geopolymer cement with soil and adding 5% of ordinary Portland cement to the mixed G plus soil blend. The X-ray fluorescence test was conducted on the Soil, QD, FA, GGBFS and OPC (Dangote brand of Portland cement) to characterize the materials based on the weight of chemical oxides each contains [10] in accordance with appropriate design standards (ASTM) E1621-13 [31, 32]). Figure 2 shows the schematic path of the methodology of the research work [10].

2.2 Experimental Methods and Data Collection and Analysis

2.2.1 Collected Database

Multiple $3 \times$ replicate experiments were conducted and an average of 99 specimens were tested and an average of each set of three (3) was estimated to have 33 outcomes on the following physical and mechanical properties of G-treated lateritic soil [33] (geopolymer cement (G) was added to the soil in the proportions of 0%, 1.5%, 2.5%, 3.5%, …, 40% as presented in the supplementary material):

- Capillary rise at 72 h curing of G-treated soil (C) %,
- Suction at 72 h curing of G-treated soil (S) %,
- Compressive strength at 72 days curing of G-treated soil (U) MPa,
- California bearing ratio at 24 h soaking of G-treated soil (B) %,
- Stiffness at 24 h soaking of G-treated soil (T) GPa, [10],
- Modulus of resilient deformation of G-treated soil (D) kg/m^2 [10],
- Capillary rise at 72 h curing of G-treated soil modified/cemented with OPC (C^) %,
- Suction at 72 h curing of G-treated soil modified/cemented with OPC (S^) %,
- Compressive strength at 72 days curing of G-treated soil modified/cemented with OPC (U^) MPa,
- California bearing ratio at 24 h soaking of G-treated soil modified/cemented with OPC (B^) %,
- Stiffness at 24 h soaking of G-treated soil modified/cemented with OPC (T^) GPa,
- Modulus of resilient deformation of G-treated soil modified/cemented with OPC (D^) kg/m^2

The 33 data items from the multiple experiments, which gave rise to five (5) input parameters and two (2) output parameters were used to in the predictive model exercise in line with the models' functional equations (Eq. 1 and 2) to predict two sets of treatment conditions (G- treated uncemented lateritic and G- treated cemented lateritic soil).

$$T; D = f(G, C, S, U, B) \tag{1}$$

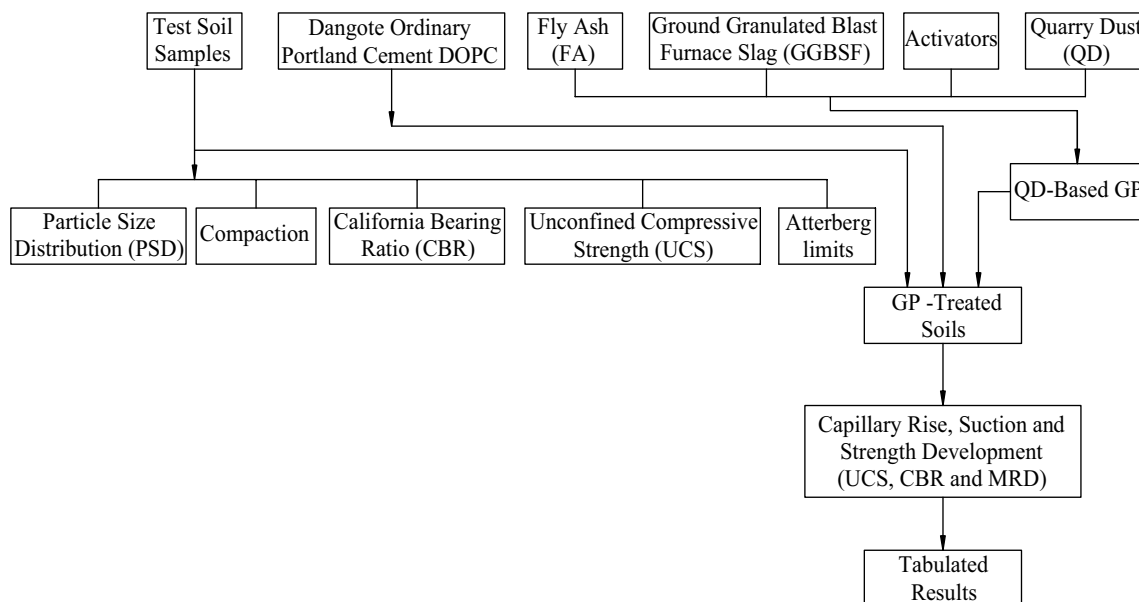$$T^\wedge; D^\wedge = f(G, C^\wedge, S^\wedge, U^\wedge, B^\wedge) \tag{2}$$

Fig. 2 Schematic path of the research methodology [10]

Table 1 Cronbach's alpha reliability statistics of uncemented input parameters (*G, C, S, U,* and *B*) with the output, *T*

Cronbach's Alpha	Cronbach's alpha based on standardized items	N of Items
0.658	0.338	6

Table 3 Reliability statistics of uncemented input parameters (*G, C, S, U,* and B) with the output, *D*

Cronbach's alpha	Cronbach's alpha based on standardized items	N of items
0.228	0.356	6

2.2.2 Statistical Reliability Analysis

The reliability or the internal consistency of the input parameters with the statistical influence on the entire system for the cases of uncemented and cemented geopolymer cement treated lateritic soil was tested and analyzed with the Cronbach's alpha reliability technique and the results are presented in Tables 1, 2, 3, 4, 5, 6, 7, 8. In Tables 1, 3, 5, and 7, the Cronbach's alpha of the consistency of the uncemented input parameters with *T* and *D* and those of the cemented input parameters with *T^* and *D^* were observed to be 0.658, 0.228, 0.581 and 0.219 respectively. According to Pallant [34], the Cronbach's alpha for any system with items greater than 10 in a scale must be ≥ 0.7 for the internal consistency between the studied parameters to be acceptable. This shows that the consistency of the parameters was not agreeable and Tables 2, 4, 6, and 8 allows an opportunity to improve the Cronbach's alpha level [34]. In the case of Table 2, the capillary rise (*C*) item alpha level shows that if *C* is removed from the entire system, the alpha level will improve from 0.658 to 0.721. However, in the cases of Tables 4, 6 and 8, the item alpha levels to be removed to improve the alpha level of the entire system are all below 0.7 and this means that for the reliability of the parameters in both cemented and uncemented cases to be consistent and influential to the output parameters, the 33 items have to be recoded or reshuffled in accordance with the requirements of Pallant [34]. Finally, the data items were reshuffled and analyzed to achieve maximum consistency as presented in Tables 1 and 2.

The reshuffled data items recorded in Tables 1 and 2 divided into training set (21 records) and validation set (12 records). Tables 9, 10, 11, 12 summarize their statistical characteristics and the Pearson correlation matrix. Finally, Fig. 3 and 4 show the histograms for both inputs and outputs.

The California bearing ratio (*B*) showed the highest means in both training and validation analysis of the items for the uncemented and cemented conditions while suction showed the least mean as shown in Tables 9 and 10. This shows the high influence of *B* on the output parameters of the models *T* and *D* and *T^* and *D^*. The unconfined compressive strength showed the least variance and standard deviation from the output parameters compared to any other parameter in both the uncemented and cemented conditions. Figure 3 and 4 show good distribution of the items consistent with the output parameters (the targets). In Tables 11 and 12, *B* and *B^* showed the highest correlation with *T* and *D* and *T^* and *D^* respectively for both cement conditions (uncemented and cemented) and this agrees with the mean, standard deviation and variance outcome of the parameters. This correlation is followed by the effect of the geopolymer cement (*G*) on the targets (*T, T^, D,* and *D^*). The third in terms of the influence in correlation is the unconfined compressive strength (*U*). Capillary rise (*C*) and suction (*S*) equally showed good correlation with the targets and this shows that all five (5) input parameters are important and should be given a chance to be eliminated in the full model exercise through step wise approach.

2.2.3 Predictive Models Research Program

Three different Artificial Intelligent (AI) techniques were used to predict the shear strength parameters of the tested soil samples. These techniques are Genetic programming (GP), Artificial Neural Network (ANN) and Polynomial Linear Regression optimized using Genetic Algorithm which is known as evolutionary polynomial regression (EPR). All the three developed models were used to predict the values of both Stiffness (*T*), Portland cemented Stiffness (*T^*), Modulus of resilient deformation (*D*) and Portland cemented

Table 2 Item total statistics of uncemented input parameters (*G, C, S, U,* and *B*) with the output, *T*

	Scale mean if item deleted	Scale variance if item deleted	Corrected item-total correlation	Squared multiple correlation	Cronbach's alpha if item deleted
G	406.1576	55,911.690	0.973	0.996	0.631
C	395.8485	64,664.627	− 0.314	0.343	0.721
S	425.3212	61,918.402	− 0.869	0.950	0.688
U	338.0303	56,700.580	0.895	0.975	0.639
B	287.6242	17,708.425	0.988	0.999	0.234
T	277.6545	17,478.421	0.989	0.999	0.234

Table 4 Item total statistics of uncemented input parameters (*G, C, S, U*, and *B*) with the output, *D*

	Scale mean if item deleted	Scale variance if item deleted	Corrected item-total correlation	Squared multiple correlation	Cronbach's alpha if item deleted
G	257.9941	14,581.215	0.959	0.998	0.045
C	247.6850	18,991.092	− 0.320	0.339	0.347
S	277.1578	17,681.898	− 0.852	0.990	0.246
U	189.8668	14,991.407	0.874	0.974	0.076
B	139.4608	615.735	0.604	0.989	− 0.290[a]
D	277.6545	17,478.421	0.919	0.968	0.234

[a]The value is negative due to a negative average covariance among items. This violates reliability model assumptions. You may want to check item codings

Table 5 Reliability statistics of cemented input parameters (*G^, C^, S^, U^*, and *B^*) with the output, *T^*

Cronbach's alpha	Cronbach's alpha based on standardized items[a]	N of items
0.581	− 0.375	6

[a]The value is negative due to a negative average covariance among items. This violates reliability model assumptions. You may want to check item codings

Table 7 Reliability statistics of cemented input parameters (*G^, C^, S^, U^*, and *B^*) with the output, D^

Cronbach's alpha	Cronbach's alpha based on standardized items[a]	N of items
0.219	-0.349	6

[a]The value is negative due to a negative average covariance among items. This violates reliability model assumptions. You may want to check item codings

Modulus of resilient deformation (*D^*) of G-treated soil using the measured geopolymer cement proportion (*G*), uncemented sets of; Capillary rise (*C*), Suction (*S*), Compressive strength (*U*) and California bearing ratio (*B*) and cemented sets of; Capillary rise (*C^*), Suction (*S^*), Compressive strength (*U^*) and California bearing ratio (*B^*). This was executed to study the influence ordinary Portland cement (OPC) addition has on the studied parameters treated with GPC and on the predicted models as a comparative study. Each model on the three developed models was based on different approach (evolutionary approach for GP, mimicking biological neurons for ANN and optimized mathematical regression technique for EPR). However, for all developed models, prediction accuracy was evaluated in terms of Sum of Squared Errors (SSE).The following section discusses the results of each model. The Accuracies of developed models were evaluated by comparing the (SSE)

between predicted and calculated shear strength parameters values. The results of all developed models are summarized in Table 4.

3 Results and Discussion

3.1 General Remarks

Table 13 shows the basic properties of the soil used in this research work. The soil was a highly plastic soil though classified as A-2-6 group soil according to AASHTO system of soil classification. The CBR (*B*) of the soil was observed to be 8%, which falls below the minimum CBR standard for soil to be used as a compacted pavement subgrade material (< 10% according to AASHTO [35]). In Fig. 5, other properties of the soil were presented. Table 14 shows the oxide

Table 6 Item total statistics of cemented input parameters (*G^, C^, S^, U^*, and *B^*) with the output, *T^*

	Scale mean if item deleted	Scale variance if item deleted	Corrected item-total correlation	Squared multiple correlation	Cronbach's alpha if item deleted
G^	667.2115	120,162.161	0.989	0.998	0.561
C^	664.3782	134,683.520	− 0.928	0.985	0.635
S^	685.0370	129,183.166	− 0.959	0.995	0.608
U^	589.0661	120,966.218	0.966	0.988	0.566
B^	538.7185	58,867.553	0.993	0.998	0.129
T^	291.4948	16,977.231	0.992	0.998	0.224

Table 8 Item total statistics of cemented input parameters ($G^\wedge$, $C^\wedge$, $S^\wedge$, $U^\wedge$, and $B^\wedge$) with the output, $D^\wedge$

	Scale mean if item deleted	Scale variance if item deleted	Corrected item-total correlation	Squared multiple correlation	Cronbach's alpha if item deleted
$G^\wedge$	272.0218	14,074.418	0.979	0.998	0.026
$C^\wedge$	269.1885	19,233.107	− 0.910	0.986	0.350
$S^\wedge$	289.8472	17,238.119	− 0.939	0.990	0.240
$U^\wedge$	193.8763	14,347.092	0.956	0.989	0.047
$B^\wedge$	143.5288	210.623	0.961	0.987	− 0.853[a]
$D^\wedge$	291.4948	16,977.231	0.975	0.972	0.224

[a]The value is negative due to a negative average covariance among items. This violates reliability model assumptions. You may want to check item codings

Table 9 Statistical analysis of collected database for uncemented condition

	(G) %	(C) %	(S) %	(U) MPa	(B) %	(T) GPa	(D) kg/m^2
Training set							
Max	0.00	0.11	0.00	0.07	0.08	0.01	0.10
Min	0.40	0.78	0.02	0.11	3.20	0.33	0.90
Avg	0.21	0.28	0.01	0.09	1.47	0.16	0.34
SD	0.13	0.17	0.01	0.01	1.19	0.12	0.26
Var	0.62	0.61	0.85	0.14	0.81	0.76	0.76
Validation set							
Max	0.03	0.14	0.00	0.07	0.08	0.02	0.12
Min	0.34	0.45	0.02	0.10	2.99	0.31	0.61
Avg	0.19	0.26	0.01	0.09	1.15	0.12	0.27
SD	0.10	0.10	0.01	0.01	1.12	0.11	0.16
Var	0.53	0.39	0.70	0.10	0.97	0.90	0.62

Table 10 Statistical analysis of collected database for cemented condition

	(G) %	(C$^\wedge$) %	(S$^\wedge$) %	(U$^\wedge$) MPa	(B$^\wedge$) %	(T$^\wedge$) GPa	(D$^\wedge$) kg/m^2
Training set							
Max	0.00	0.11	0.01	0.07	0.10	0.08	0.19
Min	0.40	0.40	0.04	0.12	3.31	0.72	0.98
Avg	0.21	0.23	0.02	0.10	1.57	0.41	0.52
SD	0.13	0.09	0.01	0.01	1.20	0.24	0.26
Var	0.62	0.41	0.40	0.12	0.76	0.58	0.50
Validation set							
Max	0.03	0.14	0.01	0.09	0.16	0.10	0.24
Min	0.34	0.40	0.04	0.11	3.07	0.68	0.72
Avg	0.19	0.23	0.02	0.10	1.24	0.35	0.43
SD	0.10	0.08	0.01	0.01	1.11	0.21	0.17
Var	0.53	0.34	0.33	0.09	0.89	0.61	0.40

composition by weight of the experimental materials, which shows that FA, QD. GGBFS and OPC had high pozzolanic ability according to the conditions of ASTM C618 [31]. It is observed in Tables 1 and 2 that the capillary rise (C) and suction (S) reduced with increased geopolymer cement (G) in both the non-cemented and cemented conditions. At 15% by weight addition of the G, the trial test cured at 72 h fell below the minimum allowable critical capillary rise of 25% proposed by Austroads [36]. This is due to increased release of Ca^{2+}, Si^{4+} and Al^{3+} by the silicate of sodium component of the activator from the FA, GGBFS and QD blend which sped up cation exchange reaction rate [16, 23]. The

Table 11 Pearson correlation matrix for the uncemented condition

	G	C	S	U	B	T	D
G	1						
C	− 0.88535	1					
S	− 0.94366	0.938107	1				
U	0.966472	− 0.92352	− 0.95875	1			
B	0.978181	− 0.78947	− 0.87628	0.903727	1		
T	0.981187	− 0.79833	− 0.88334	0.909506	0.999309	1	
D	0.875373	− 0.64864	− 0.68157	0.797245	0.90261	0.902738	1

Table 12 Pearson correlation matrix for cemented condition

	G	C^	S^	U^	B^	T^	D^
G	1						
C^	− 0.95432	1					
S^	− 0.97969	0.978052	1				
U^	0.983593	− 0.91982	− 0.96911	1			
B^	0.981371	− 0.90099	− 0.93653	0.95613	1		
T^	0.991227	− 0.93746	− 0.9683	0.968506	0.992826	1	
D^	0.970186	− 0.88781	− 0.91628	0.945919	0.973241	0.963394	1

substantial reduction in suction with increased addition of G was due to the ability of G to react and reduce the porosity of the G-treated uncemented and cemented soil. The UCS (U) also behaved in an improved consistency with increased addition of G due to the increased Ca^{2+} release [10]. This equally increased the intergranular contact between the soil structures and consequently reduced the porosity in the treated soil thereby increasing densification, flocculation and strength gain, which is translated as improved USC (U). Figures 6 and 7 show the effect of the G on stiffness (T) and the modulus of resilient deformation (D) of both uncemented and cemented lateritic soil. It can be observed that the T and D improved substantially with increased G and with 5% addition of cement on the second case. This serves as a good data to predict the behavior of stabilized lateritic subgrade soils for sustainable construction.

3.2 Prediction of Output Parameters (T, T^, D, and D^)

3.2.1 Model (1): Using (GP) Technique

The developed GP model has only two levels of complexity. The population size, survivor size and number of generations were 30,000, 10,000 and 50 respectively. Equation (3) and (4) present the output formulas for (T) and (D) respectively, while Figs. 10a and 12a show their fitness respectively. The

average error % of total set for (T) and (D) are (2.9%) and (6.9%), respectively, while the (R^2) values are (0.999) and (0.993), respectively.

Equation (5), (6) present the output formulas for (T^) and (D^) respectively, while Figs. 11a and 13a show their fitness respectively. The average error % of total set for (T^) and (D^) are (6.9%) and (6.5%) respectively, while the (R^2) values are (0.990) and (0.980) respectively, which agrees with El-Bosraty et al. [37] and Ebid [38].

$$T = \frac{U + B}{10} \tag{3}$$

$$D = \frac{1 + U}{8.25 - 2.2B} \tag{4}$$

$$T^\wedge = 4.5\ U^\wedge + 0.16\ B^\wedge - 0.27 \tag{5}$$

$$D^\wedge = \frac{\left(G/C^\wedge\right) + 2\ e^{3.66\ G^\wedge}}{13} + 0.055 \tag{6}$$

3.2.2 Model (2): Using (ANN) Technique

A back propagation ANN with one hidden layer and nonlinear activation function (Sigmoid) was used to predict both Stiffness (T) and modulus of resilient deformation (D). The
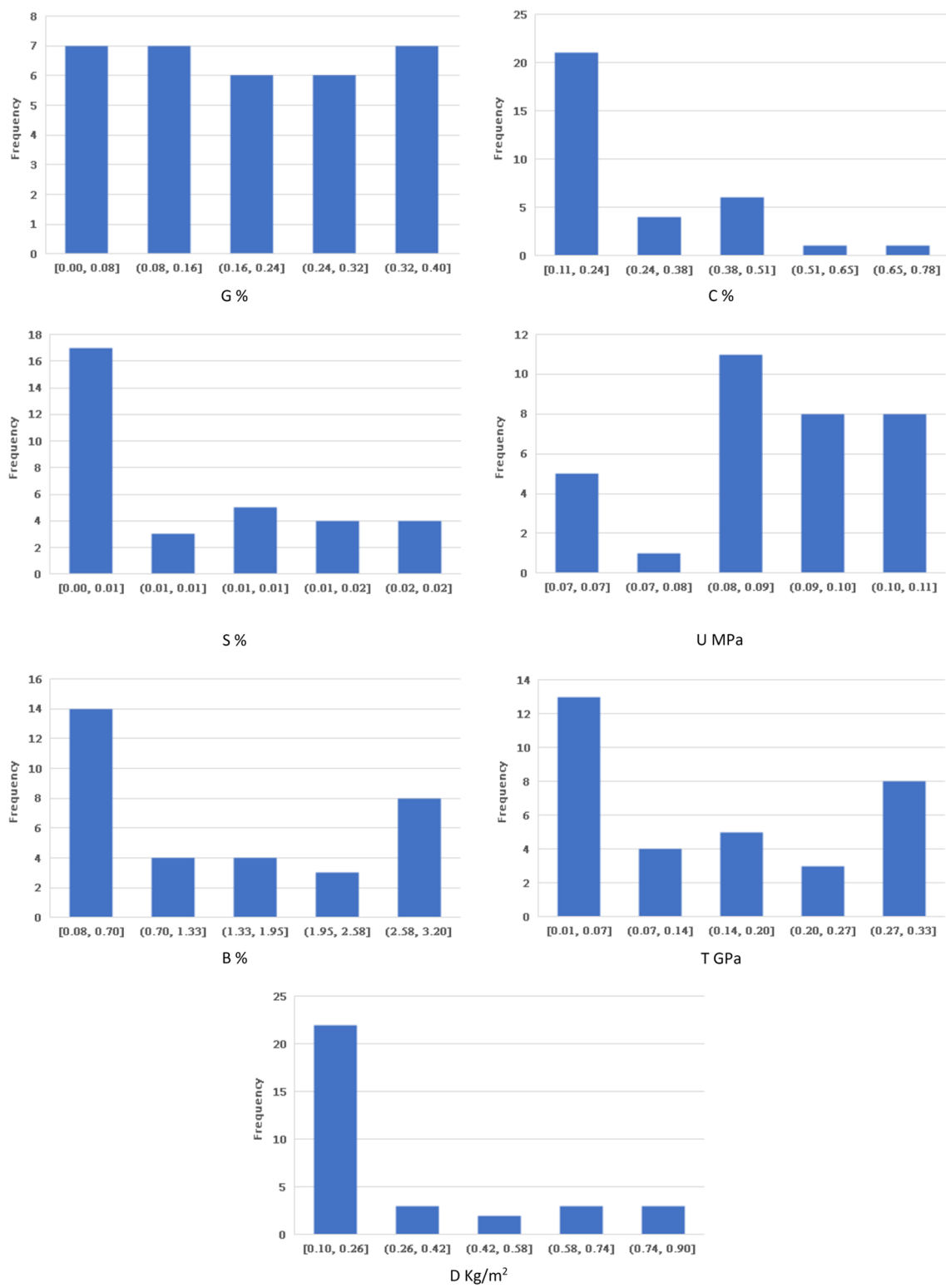
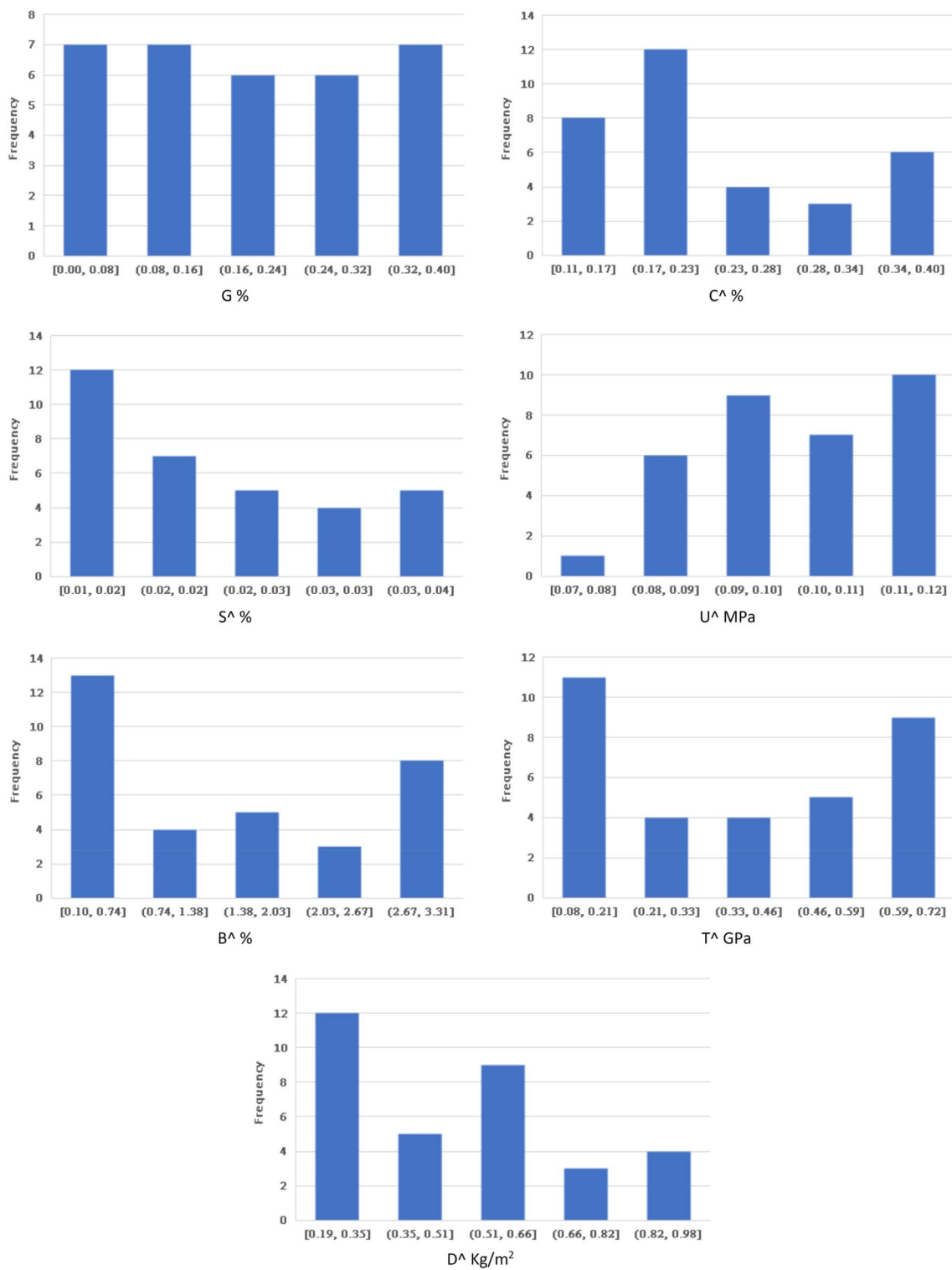**Fig. 3** Distribution histograms for inputs and outputs

Fig. 4 Distribution histograms for inputs and outputs

Table 13 Basic properties of the lateritic soil

Property	%Passing 200 sieve	NMC, %	W_L, %	W_P, %	I_P, %	SG	MDD, g/cm^3	OMC, %	CBR (B), %	AASHTO
Result	5.4	13	40	18	22	2.6	1.83	16.2	8	A-2-6
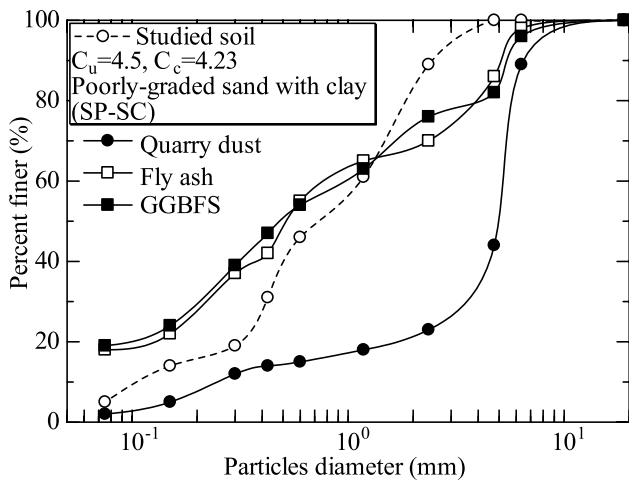
Fig. 5 Grain size distributions of materials [10]

GP is geopolymer

Fig. 6 Subgrade reference soil stiffness of uncemented and cemented lateritic soil treated with geopolymer cement (GPC or GP) [10].*GP is geopolymer

used networks layout and their connation weights are illustrated in Fig. 8. Equations (7) and (9) present the equivalent functions of the developed ANN models. The average error % of total dataset for these equations are (3.6%) and (6.0%) and the (R^2) values are (0.998) and (0.993) respectively. The relations between calculated and predicted values are shown in Figs. 10b and 12b.

A back propagation ANN with one hidden layer and non-linear activation function (Sigmoid) was used to predict both stiffness ($T^\wedge$) and modulus of resilient deformation ($D^\wedge$). The used networks layout and their connation weights are illustrated in Fig. 9. Equations (15) and (16) present the equivalent functions of the developed ANN models. The average error % of total dataset for these equations are (3.1%) and (5.2%) and the (R^2) values are (0.997) and (0.987) respectively, which agrees with El-Bosraty et al. [37] and Ebid [38]. The relations between calculated and predicted values are shown in Figs. 11b and 13b.
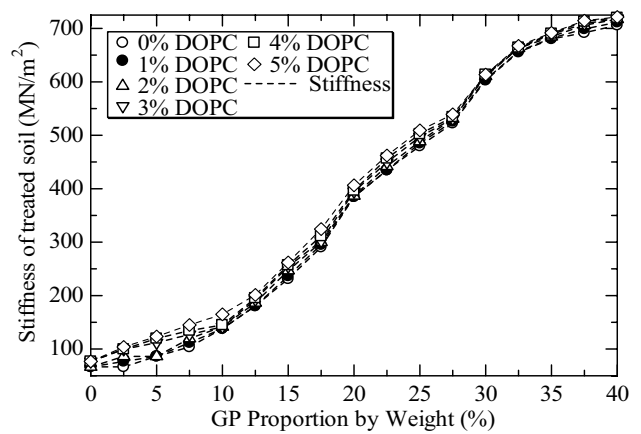
$$T = 0.01 + \frac{0.32}{1 + e^{-Y1}} \tag{7}$$

GP is geopolymer

Fig. 7 Modulus of Resilient Deformation (D) of uncemented and cemented lateritic soil treated with geopolymer cement (GPC or GP) [10]. *GP is geopolymer

$$Y1 = 0.048 + \frac{6.26}{1 + e^{-X1}} - \frac{3.00}{1 + e^{-X2}} \tag{8}$$

Table 14 Chemical oxides composition of experimental materials [10]

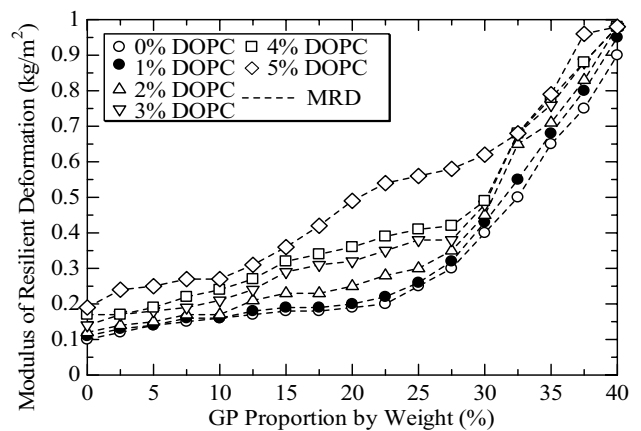| Materials	Oxides composition (content wt %)												
	SiO_2	Al_2O_3	CaO	Fe_2O_3	MgO	K_2O	Na_2O	TiO_2	LOI	P_2O_5	SO_3	IR	Free CaO
Soil	77.73	16.65	1.42	3.22	0.07	0.89	0.02	-	-	-	-	-	-
QD	63.48	17.72	5.56	1.77	4.65	2.76	0.01	3.17	0.88	-	-	-	-
FA	63.45	4.14	12.11	1.23	0.78	1.09	0.01	1.78	1.89	0.71	0.11	-	0.03
GGBFS	33.45	12.34	42.10	0.05	11.45	–	-	-	0.21	-	-	-	0.40
OPC	21.45	4.45	63.81	3.07	2.42	0.83	0.20	0.22	0.81	0.11	2.46	0.16	0.64

*IR is insoluble residue; LOI is loss on ignition, FA, fly ash

QD, quarry dust; GGBFS, ground granulated blast furnace slag; DOPC, Dangote ordinary portland cement or OPC; ordinary portland cement

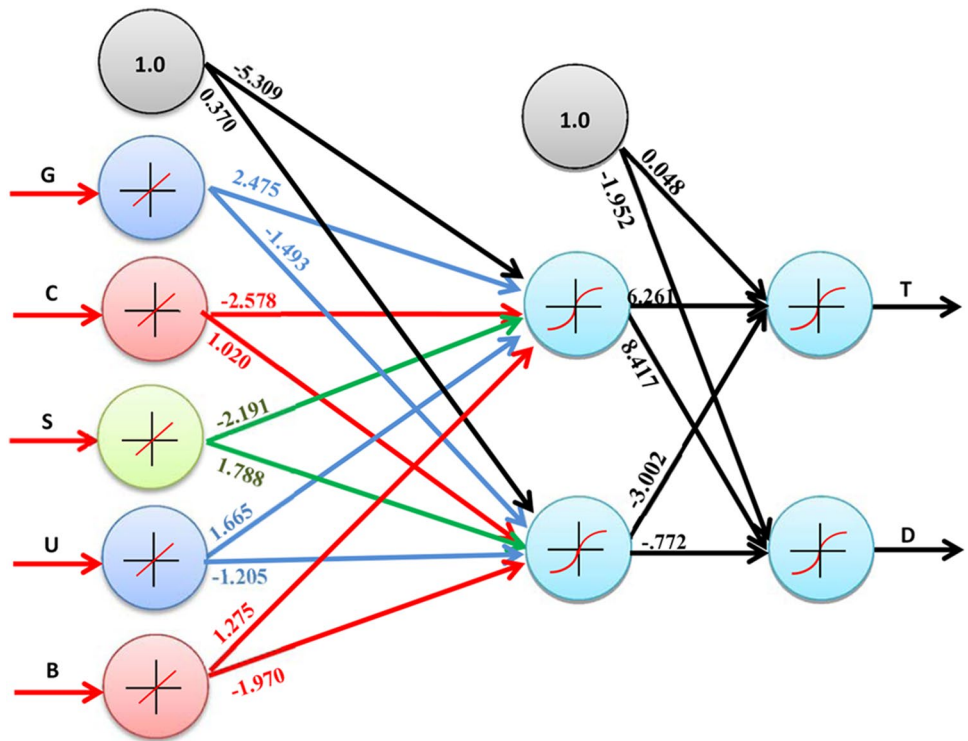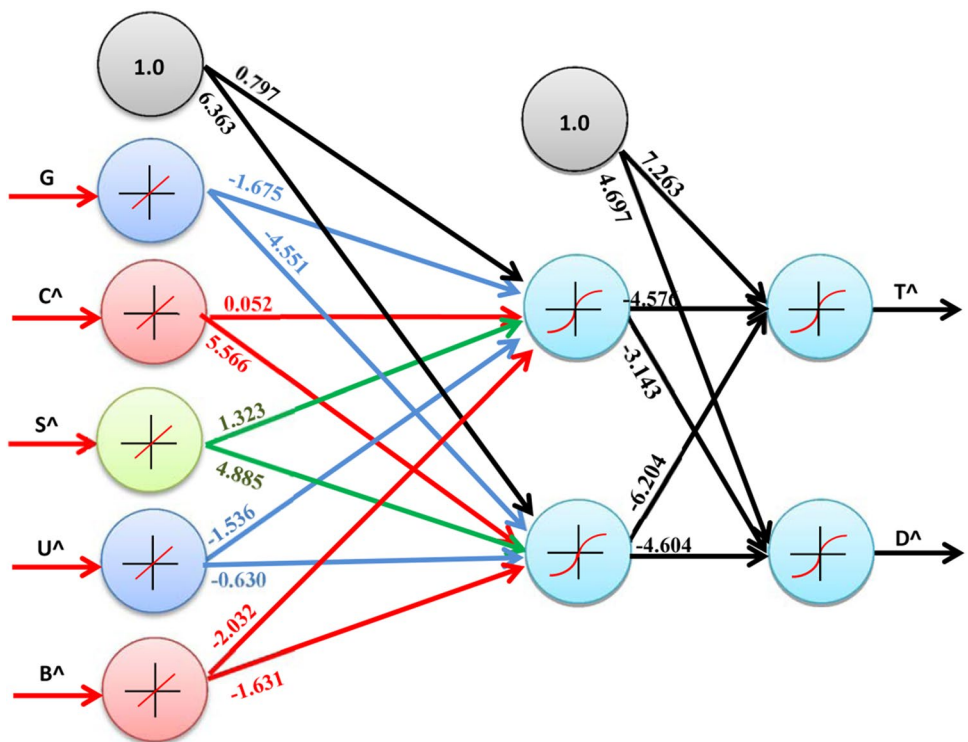**Fig. 8** Layout for the developed ANN's and their connection weights

Fig. 9 Layout for the developed ANN's and their connection weights

$$D = 0.10 + \frac{0.80}{1 + e^{-Y2}} \tag{9}$$

$$Y2 = -1.95 + \frac{8.42}{1 + e^{-X1}} - \frac{0.77}{1 + e^{-X2}} \tag{10}$$

$$X1 = -5.31 + 2.48G' - 2.58C' - 2.19S' + 1.67U' + 1.28B' \tag{11}$$

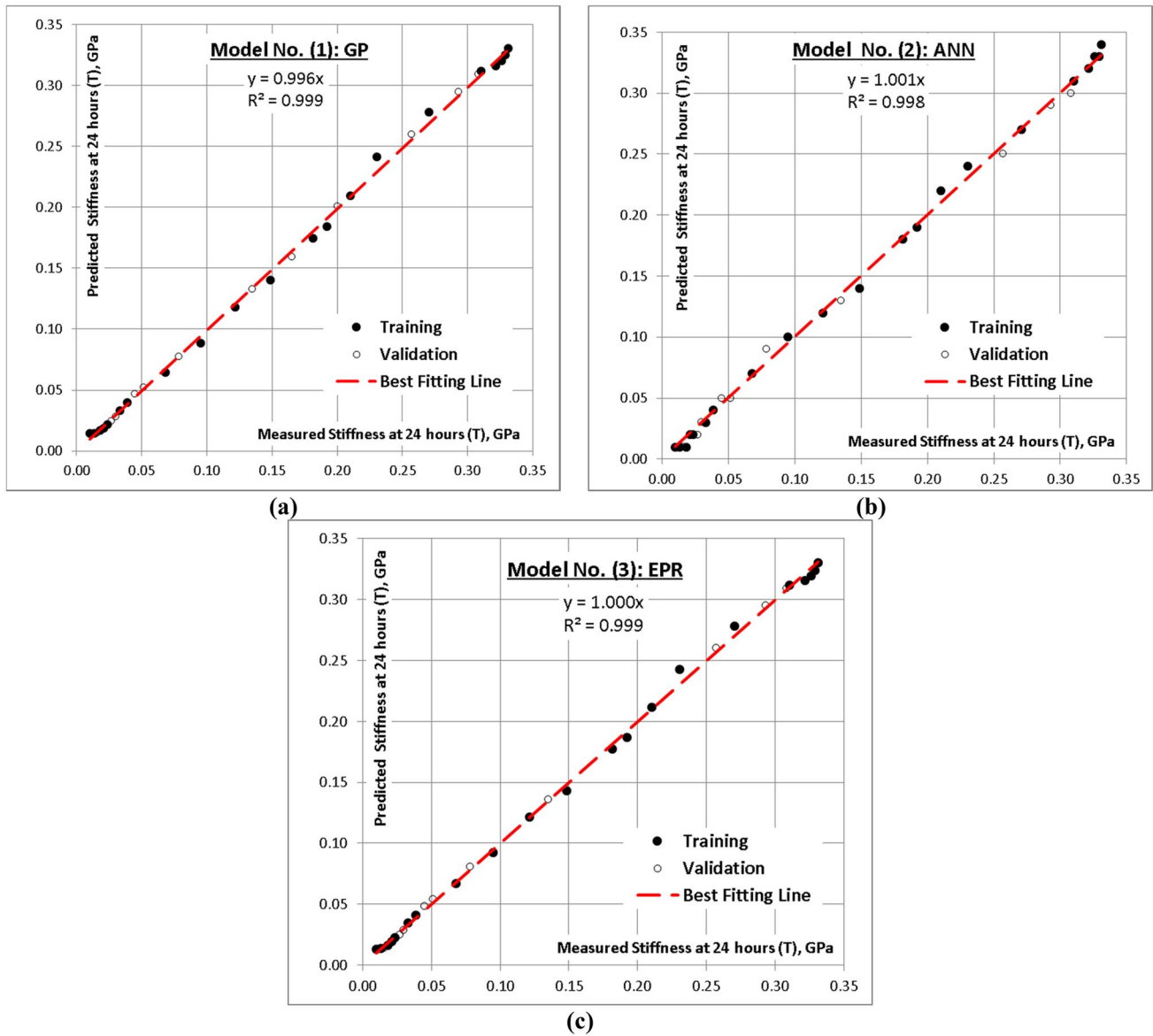$$X2 = 0.37 - 1.49\,G' + 1.02\,C' + 1.79\,S' - 1.21\,U' - 1.97\,B' \tag{12}$$

Fig. 10 Relation between predicted and calculated (*T*); **a** GP, **b** ANN, and **c** EPR values using the developed models

$$G' = \frac{G}{0.40}; C' = \frac{C - 0.11}{0.67}; S' = \frac{S - 0.001}{0.02}; U' = \frac{U - 0.065}{0.04}; B' = \frac{B - 0.08}{3.12} \tag{13}$$

$$T^\wedge = 0.077 + \frac{0.645}{1 + e^{-Y1}} \tag{14}$$

$$Y1 = 7.263 - \frac{4.576}{1 + e^{-X1}} - \frac{6.204}{1 + e^{-X2}} \tag{15}$$

$$D^\wedge = 0.190 + \frac{0.790}{1 + e^{-Y2}} \tag{16}$$

$$Y2 = 4.697 - \frac{3.143}{1 + e^{-X1}} - \frac{4.604}{1 + e^{-X2}} \tag{17}$$

$$X1 = 0.797 - 1.675\,G' + 0.052\,C' + 1.323\,S' - 1.536\,U' - 2.032\,B' \tag{18}$$

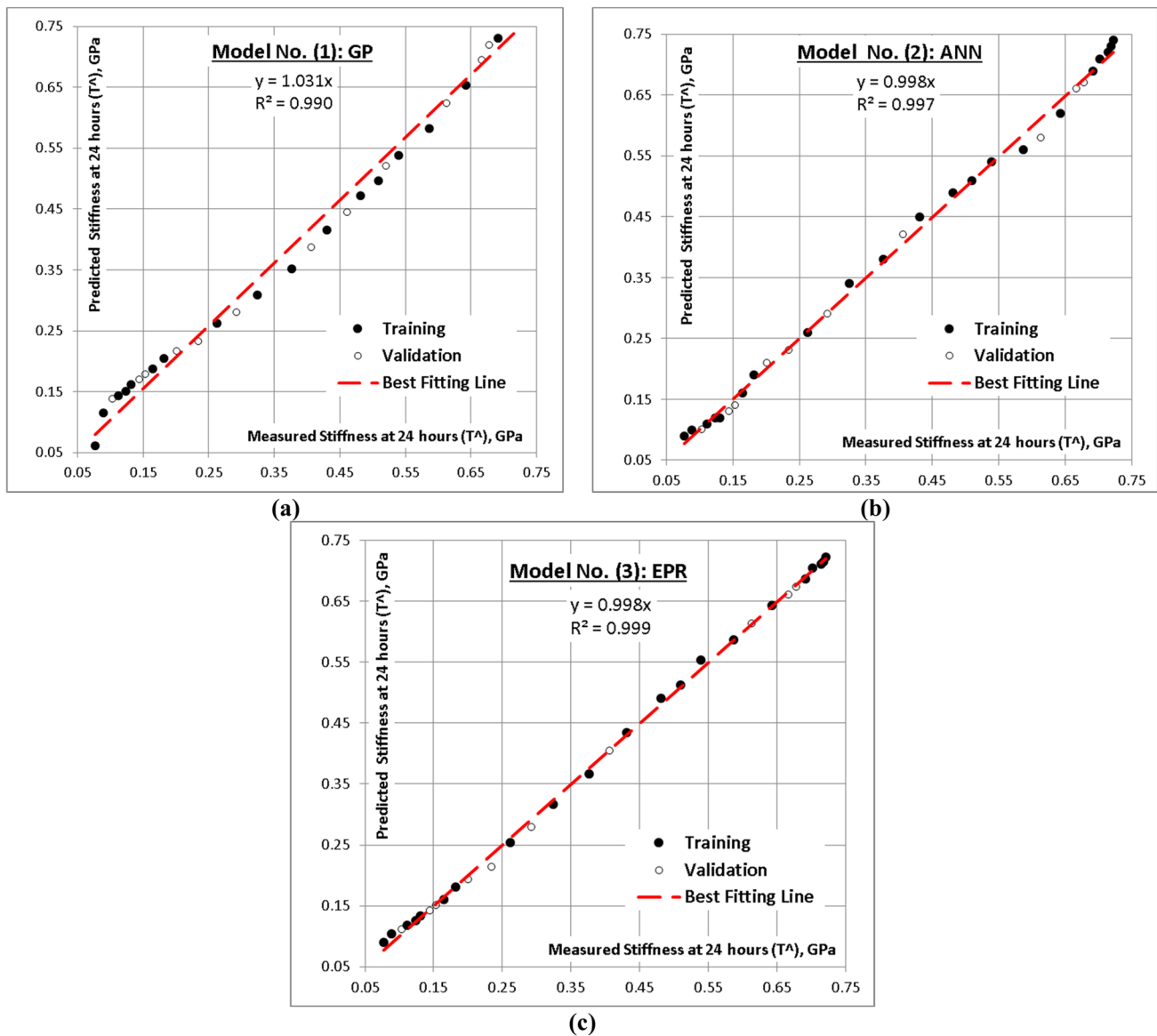$$X2 = 6.363 - 4.551G' + 5.566C' + 4.885S' - 0.630U' - 1.631B' \tag{19}$$

Fig. 11 Relation between predicted and calculated ($T^\wedge$); **a** GP, **b** ANN, and **c** EPR values using the developed models

$$G' = \frac{G}{0.40}; \; C' = \frac{C^\wedge - 0.11}{0.29}; \; S' = \frac{S^\wedge - 0.011}{0.026}; \; U' = \frac{U^\wedge - 0.07}{0.045}; \; B' = \frac{B^\wedge - 0.10}{3.21} \tag{20}$$

3.2.3 Model (3): Using (EPR) Technique

Finally, to predict (T) and (D) values, the developed EPR model was limited to quadratic level, for five inputs, there are 21 possible terms $\left(\sum_{i=1}^{i=5} \sum_{j=1}^{j=5} X_i.X_j + \sum_{i=1}^{i=5} X_i + C \right)$. GA technique was applied on these 21 terms to select the most

effective 3 terms. On the other hand, to predict the values of ($T^\wedge$) and ($D^\wedge$) the developed EPR model was limited to cubic level, for five inputs, there are 56 possible terms $\left(\sum_{i=1}^{i=5} \sum_{j=1}^{j=5} \sum_{k=1}^{k=5} X_i.X_j.X_k + \sum_{i=1}^{i=5} \sum_{j=1}^{j=5} X_i.X_j + \sum_{i=1}^{i=5} X_i + C. \right)$ GA technique was applied on these 56 terms to select the most effective 4 terms. The outputs are illustrated in Eqs. (21)–(24) and their fitness are shown in Figs. 10c, 11c, 12c, 13c. The average error % (SSE) and (R^2) values in the
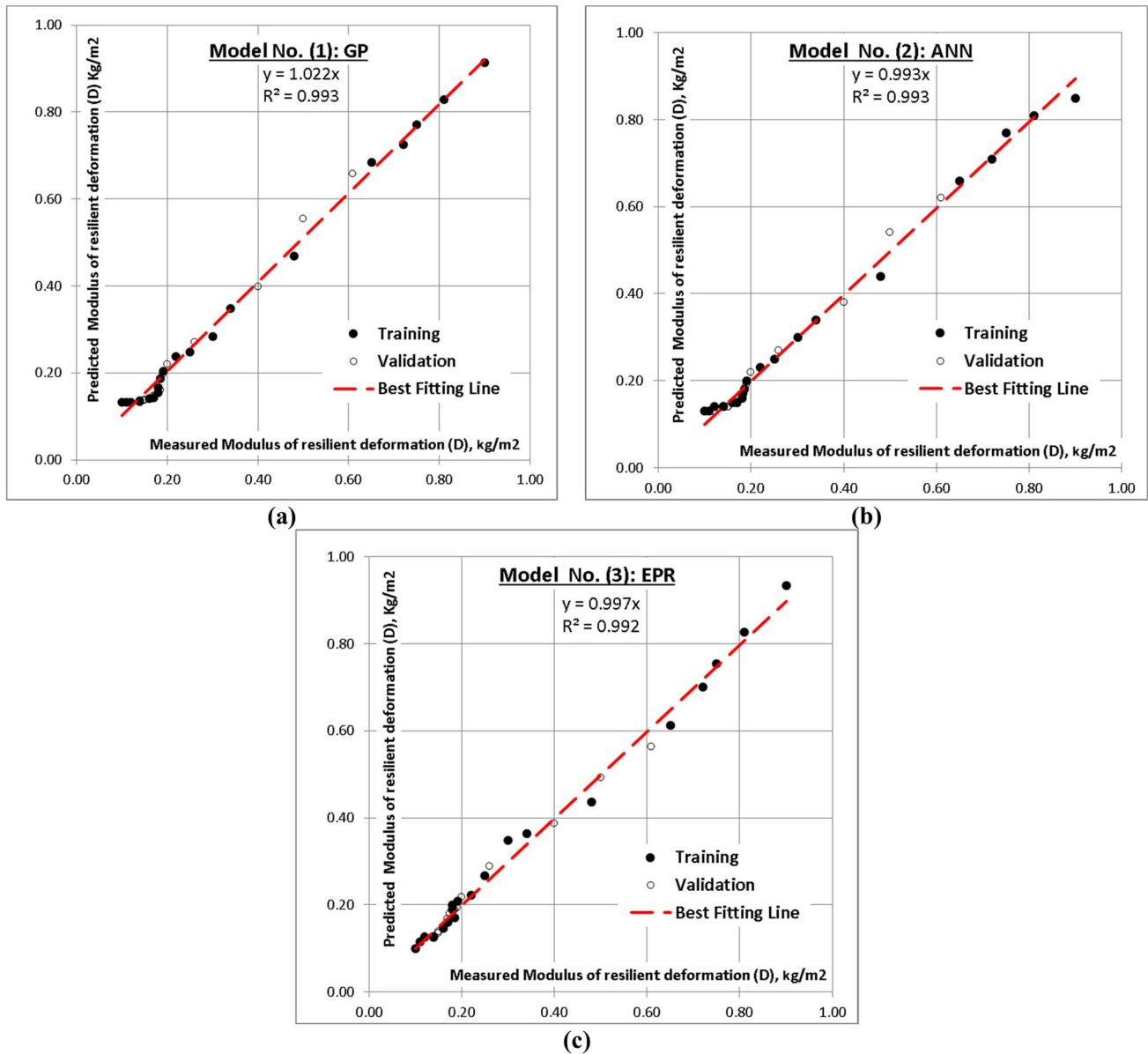
Fig. 12 Relation between predicted and calculated (D); **a** GP, **b** ANN, and **c** EPR values using the developed models

case of uncemented model were improved to (2.6%)–(0.999) and (6.7%)–(0.992) for the total datasets respectively while for the case of the cemented model, the average error% (SSE) and (R^2) values were improved to (2.1%)–(0.999) aand (4.6%)–(0.990) for the total datasets respectively, which agrees with El-Bosraty et al. [37] and Ebid [38].

$$T = 0.098B - 0.591S + 0.0179 \tag{21}$$

$$D = 6.865G^2 - 0.913C \cdot B + 0.157 \tag{22}$$

$$T^\wedge = 0.068 + 3.31\,U^\wedge \cdot B^\wedge - 0.055\,B^{\wedge 2} \tag{23}$$

$$D^\wedge = 0.094 + 23.1\,S^\wedge \cdot B^\wedge + \left(0.249\,G - 8.52\,S^\wedge\right)B^{\wedge 2} \tag{24}$$

The general summary of the performance of the models for cemented and uncemented predicted parameters of the geopolymer cement treated lateritic soil is presented in Tables 15, 16.
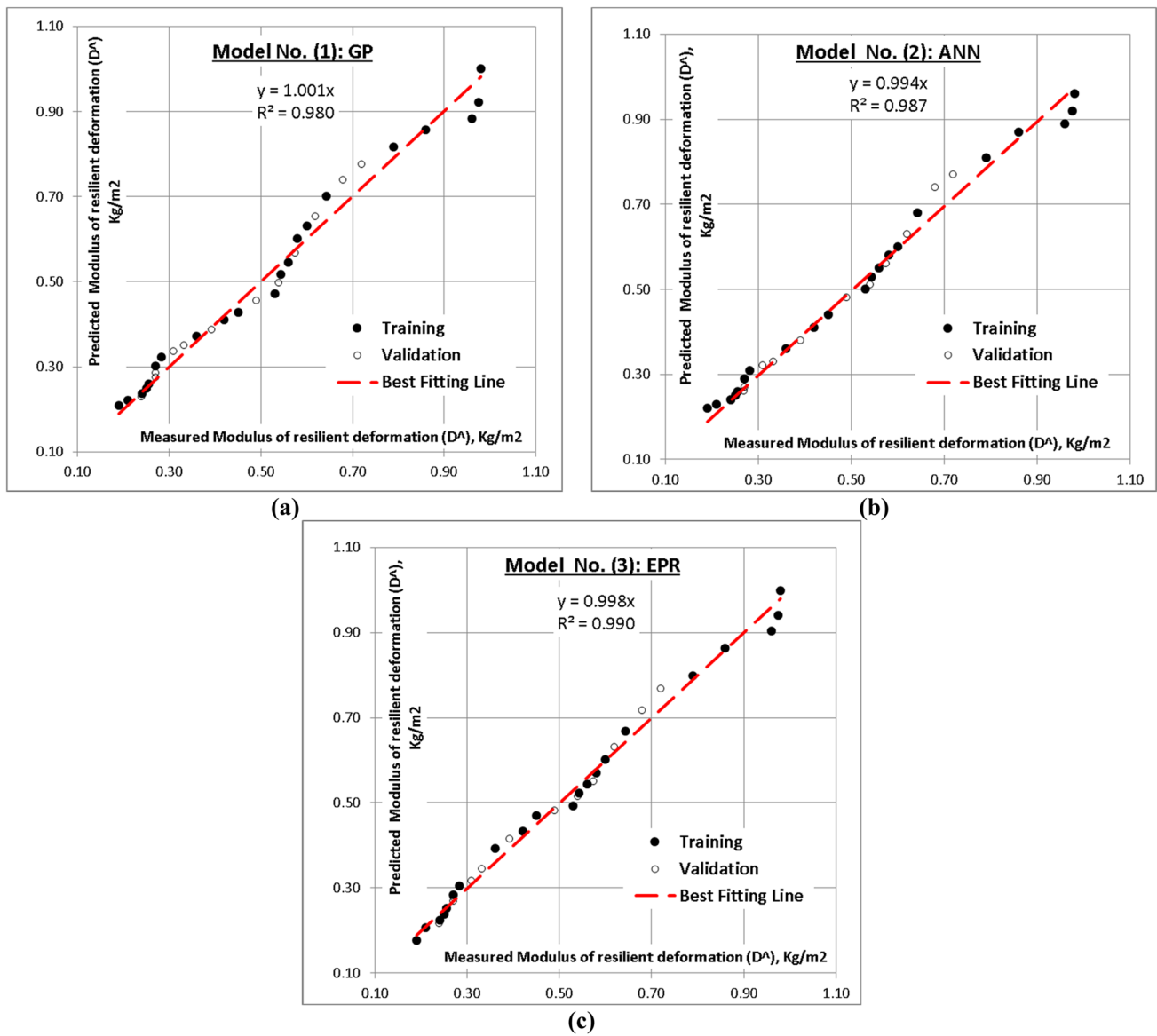
Fig. 13 Relation between predicted and calculated ($D^\wedge$); **a** GP, **b** ANN, and **c** EPR values using the developed models

4 Conclusions

This research presents three models using three artificial intelligent (AI) techniques (GP, ANN and EPR) to predict values of both stiffness (T) and modulus of resilient deformation (D) of G-treated soil using the measured geopolymer cement proportion (G), and the uncemented parameters; capillary rise (C), Suction (S), Compressive strength (U) and California bearing ratio (B) and the cemented parameters; capillary rise ($C^\wedge$), suction ($S^\wedge$), compressive strength ($U^\wedge$) and California bearing ratio ($B^\wedge$). From the performance accuracy evaluation conducted on the proposed models, the following can be concluded (Tables 17, 18);

Table 15 Performance accuracies of developed models for the uncemented parameters

Soil propriety	Technique	Developed Eq.	Error %	R^2
T	GP	Equation (3)	2.9	0.999
	ANN	Equation (7)	3.6	0.998
	EPR	Equation (21)	2.6	0.999
D	GP	Equation (4)	6.9	0.993
	ANN	Equation (9)	6.0	0.993
	EPR	Equation (23)	6.7	0.992

Table 16 Performance accuracies of developed models for the cemented parameters

Soil propriety	Technique	Developed Eq	Error %	R^2
$T\char`^$	GP	Equation (5)	6.9	0.990
	ANN	Equation (14)	3.1	0.997
	EPR	Equation (22)	2.1	0.999
$D\char`^$	GP	Equation (6)	6.5	0.980
	ANN	Equation (16)	5.2	0.987
	EPR	Equation (24)	4.6	0.990

- Prediction accuracies of (T) for all models are so close (between 96.4 and 97.4%),which gives an advantage to the simplest model(GP model), while the prediction accuracies of (D) are ranged between 93.1 and 94.0% and the simplest model equation is the (EPR) model. Also, prediction accuracies of ($D\char`^$) for all models are so close (between 94.5 and 95.5%), which gives an advantage to the simplest model equation (GP model), while the prediction accuracies of ($T\char`^$) are ranged between 93.0 and 98.0% and the simplest model equation is the (EPR) model.
- (GP) model illustrated that both (T) and (D) values are governed by (B) and (U). On the other hand, the (EPR)

Table 17 The used database

G	C	S	U	B	T	D
%	%	%	MPa	%	GPa	kg/m²
Training set						
0.385	0.121	0.0017	0.1042	3.145	0.3291	0.81
0.21	0.211	0.005	0.0902	1.31	0.1486	0.191
0.05	0.44	0.017	0.07	0.12	0.021	0.14
0.035	0.445	0.019	0.0685	0.098	0.0183	0.12
0.4	0.11	0.001	0.105	3.2	0.331	0.9
0.1	0.35	0.013	0.084	0.25	0.033	0.16
0	0.78	0.021	0.065	0.08	0.01	0.1
0.06	0.431	0.015	0.076	0.141	0.0234	0.14
0.315	0.164	0.0029	0.0971	2.685	0.2705	0.48
0.015	0.58	0.021	0.066	0.081	0.0134	0.11
0.275	0.18	0.003	0.095	2	0.21	0.3
0.25	0.2	0.003	0.094	1.75	0.192	0.25
0.35	0.14	0.002	0.1	3.02	0.31	0.65
0.115	0.312	0.012	0.0849	0.311	0.0387	0.17
0.29	0.175	0.003	0.0954	2.32	0.2305	0.34
0.375	0.13	0.002	0.103	3.1	0.326	0.75
0.365	0.133	0.0021	0.101	3.06	0.3215	0.72
0.185	0.222	0.0055	0.0871	1.095	0.1214	0.185
0.15	0.24	0.01	0.085	0.56	0.068	0.18
0.235	0.208	0.0034	0.093	1.654	0.1813	0.22
0.175	0.23	0.006	0.086	0.8	0.095	0.18
Validation set						
0.3	0.17	0.003	0.096	2.5	0.257	0.4
0.085	0.387	0.014	0.083	0.196	0.0301	0.15
0.2	0.21	0.005	0.088	1.24	0.135	0.19
0.34	0.142	0.002	0.0992	2.99	0.3084	0.61
0.325	0.15	0.002	0.098	2.85	0.293	0.5
0.075	0.42	0.015	0.082	0.16	0.027	0.15
0.135	0.26	0.0108	0.0851	0.434	0.0515	0.175
0.125	0.28	0.011	0.085	0.38	0.045	0.17
0.025	0.45	0.02	0.068	0.08	0.016	0.12
0.16	0.231	0.0075	0.0858	0.686	0.0785	0.185
0.225	0.21	0.004	0.092	1.5	0.165	0.2
0.26	0.191	0.0031	0.0947	1.91	0.2004	0.26

Table 18 The used database

G	C^	S^	U^	B^	T^	D^
%	%	%	MPa	%	GPa	kg/m²
Training set						
0.385	0.125	0.0115	0.11425	3.275	0.71805	0.975
0.21	0.19	0.0181	0.0986	1.5102	0.43076	0.53
0.05	0.38	0.032	0.086	0.21	0.12352	0.25
0.035	0.395	0.033	0.0854	0.183	0.11144	0.241
0.4	0.11	0.011	0.115	3.31	0.72144	0.98
0.1	0.3	0.028	0.09	0.33	0.16495	0.27
0	0.35	0.037	0.07	0.1	0.07683	0.19
0.06	0.366	0.0312	0.0874	0.24	0.1309	0.255
0.315	0.153	0.0133	0.1095	2.695	0.6429	0.643
0.015	0.37	0.037	0.0805	0.14	0.08865	0.21
0.275	0.17	0.016	0.105	2.1	0.53918	0.58
0.25	0.18	0.017	0.102	1.92	0.50913	0.56
0.35	0.13	0.013	0.112	3.1	0.69181	0.79
0.115	0.268	0.0261	0.091	0.404	0.1815	0.282
0.29	0.171	0.0153	0.1061	2.3405	0.5864	0.6
0.375	0.13	0.012	0.114	3.26	0.71445	0.96
0.365	0.13	0.0122	0.1135	3.205	0.7014	0.86
0.185	0.201	0.0202	0.0961	1.184	0.37643	0.45
0.15	0.23	0.024	0.094	0.68	0.26201	0.36
0.235	0.184	0.0172	0.1013	1.788	0.4813	0.543
0.175	0.21	0.021	0.095	0.95	0.32453	0.42
Validation set						
0.3	0.17	0.014	0.107	2.57	0.61358	0.62
0.085	0.321	0.0295	0.0891	0.3	0.1541	0.271
0.2	0.19	0.019	0.098	1.35	0.40637	0.49
0.34	0.14	0.0131	0.11085	3.065	0.6785	0.72
0.325	0.14	0.013	0.11	2.93	0.66728	0.68
0.075	0.34	0.031	0.088	0.27	0.14507	0.27
0.135	0.245	0.0247	0.0931	0.523	0.2346	0.332
0.125	0.25	0.025	0.092	0.45	0.20117	0.31
0.025	0.4	0.035	0.085	0.16	0.10379	0.24
0.16	0.22	0.0231	0.0943	0.783	0.2929	0.392
0.225	0.19	0.018	0.1	1.65	0.46206	0.54
0.26	0.176	0.0161	0.1038	2.017	0.52065	0.575

model showed that they mainly depend on (*B*) besides (*S*) and (*G*). On the second case (cemented), both (GP) and (EPR) models illustrated that both (*T*^) values are governed by (*B*^) and (*U*^). On the other hand, the (*D*^) values are mainly dependence on (*G*) besides (*B*^), (*S*^) and (*C*^).

- Although the ANN model had very simple configurations (one hidden layer with two neurons and sigmoid activation function), but it was still able to capture the relationship between the inputs and the outputs accurately. It almost shared the same accuracy level with (GP) and (EPR) models.

- Since the three models share almost the same level of accuracy, (ANN) models are considered the worst of them due to its complicated equivalent equations.
- GA technique successfully reduced all possible polynomial terms of conventional PLR the only effective terms without significant impact on its accuracy.
- Like any other intelligent regression technique, the generated formulas are valid within the considered range of parameter values, beyond this range; the prediction accuracy should be verified.
- Prediction accuracies of (*T*) for all models are so close (between 96.4 and 97.4%),which gives an advantage to the simplest model(GP model), while the prediction

accuracies of (*D*) are ranged between 93.1 and 94.0% and the simplest model equation is the (EPR) model. Also, prediction accuracies of (*D^*) for all models are so close (between 94.5 and 95.5%), which gives an advantage to the simplest model equation (GP model), while the prediction accuracies of (*T^*) are ranged between 93.0 and 98.0% and the simplest model equation is the (EPR) model.

- (GP) model illustrated that both (*T*) and (*D*) values are governed by (*B*) and (U). On the other hand, the (EPR) model showed that they mainly depend on (*B*) besides (*S*) and (*G*). On the second case (cemented), both (GP) and (EPR) models illustrated that both (*T^*) values are governed by (*B^*) and (*U^*). On the other hand, the (*D^*) values are mainly dependence on (*G*) besides (*B^*), (*S^*) and (*C^*).

- Although the ANN model had very simple configurations (one hidden layer with two neurons and sigmoid activation function), but it was still able to capture the relationship between the inputs and the outputs accurately. It almost shared the same accuracy level with (GP) and (EPR) models.

- Since the three models share almost the same level of accuracy, (ANN) models are considered the worst of them due to its complicated equivalent equations.

- GA technique successfully reduced all possible polynomial terms of conventional PLR the only effective terms without significant impact on its accuracy.

- Like any other intelligent regression technique, the generated formulas are valid within the considered range of parameter values, beyond this range; the prediction accuracy should be verified.

Declarations

Conflict of Interest The authors declare no conflict of interests regarding the publication of this research work.

References

1. Tanyu, B. F., Aydilek, A. H., Lau, A. W., Edil, T. B., & Benson, C. H. (2013). Laboratory evaluation of geocell-reinforced gravel subbase over poor subgrades. *Geosynthetics International, 20*(2), 47–61.

2. Tingle, J., & Jersey, S. (2005). Cyclic plate load testing of geosynthetic-reinforced unbound aggregate roads. *Transportation Research Record, 1936*, 60–69.

3. Tang, X., Stoffels, S., & Palomino, A. (2013). Resilient and permanent deformation characteristics of unbound pavement layers modified by geogrids. *Transportation Research Record: Journal of the Transportation Research Board., 2369*, 3–10. https://doi.org/10.3141/2369-01

4. Tanyu, B. F., Abbaspour, A., Alimohammadlou, Y., & Tecuci, G. (2021). Landslide susceptibility analyses using Random Forest, C4.5, and C5.0 with balanced and unbalanced datasets. *CATENA, 203*, 105355. https://doi.org/10.1016/j.catena.2021.105355.

5. Divine, O. (1998). Dynamic Interaction between vehicles and infrastructure experiment: Technical Report, Organization for Economic Co-operation and Development, Road Transport Research, Scientific Expert Group, Paris.

6. Zhang, J., Peng, J., Zhang, A., & Jue, L. (2020). Prediction of permanent deformation for subgrade soils under traffic loading in Southern China. *International Journal of Pavement Engineering*. https://doi.org/10.1080/10298436.2020.1765244

7. Venkatesh, N., Heeralal, M., & Pillai, R. J. (2020). Resilient and permanent deformation behaviour of clayey subgrade soil subjected to repeated load triaxial tests. *European Journal of Environmental and Civil Engineering, 24*(9), 1414–1429. https://doi.org/10.1080/19648189.2018.1472041

8. Al-Qadi, I., Xie, W., & Elseifi, M. A. (2008). Frequency determination from vehicular loading time pulse to predict appropriate complex modulus in MEPDG. *Journal Association of Asphalt Paving Technologists AAPT, 77*, 2.

9. Barksdale, R. D., Itani S. Y. (1989). Influence of aggregate shape on base behavior, transportation research record 1227, Transportation research Board, National Research Council, Washington.

10. Van Bui, D., Onyelowe, K. C., & Van Nguyen, M. (2018). Capillary rise, suction (absorption) and the strength development of HBM treated with QD base Geopolymer. *International Journal of Pavement Research and Technology*. https://doi.org/10.1016/j.ijprt.2018.04.003

11. Cardone, D. C. F., Cerni, G., Virgili, A., & Camilli, S. (2011). Characterization of permanent deformation behaviour of unbound granular materials under repeated triaxial loading. *Construction and Building Materials, 28.1*, 79–87.

12. Chen, Q., Hanandeh, S., Abu-Farsakh, M., & Mohammad, L. (2017). Performance evaluation of full-scale geosynthetic reinforced flexible pavement. *Geosynthetics International., 25*, 1–11. https://doi.org/10.1680/jgein.17.00031

13. Sahaf, A., Dariush, M., & Moazami, D. (2014). Effect of stiffness modulus and dynamic loading on pavement subgrade. *Journal of Civil Engineering and Construction Technology., 5*, 30–34. https://doi.org/10.5897/JCECT2014.0310

14. Shahin, M. A. (2015). Genetic programming for modelling of geotechnical engineering systems. In: Gandomi A., Alavi A., Ryan C. (eds.) *Handbook of Genetic Programming Applications*. Springer, Cham. https://doi.org/10.1007/978-3-319-20883-1_2.

15. Javdanian, H. (2017). The effect of geopolymerization on the unconfined compressive strength of stabilized fine-grained soils. *International Journal of Engineering, Transactions B: Applications, 30*, 1673–1680. https://doi.org/10.5829/ije.2017.30.11b.07

16. Onyelowe, K. C., Onyia, M. E., Van Bui, D., Firoozi, A. A., Uche, O. A., Kumari, S., Oyagbola, I., Amhadi, T., & Dao-Phuc, L.

(2021). Shrinkage parameters of modified compacted clayey soil for sustainable earthworks. *Jurnal Kejuruteraan, 33*(1), 137–144. https://doi.org/10.17576/jkukm-2020-33(1)-13

17. Koza, J., & Poli, R. (2005) A genetic programming tutorial. In: E. Burke (Ed.) Introductory tutorials in optimization, search and decision support, Chapter 8. http://www.genetic-programming.com/jkpdf/burke2003tutorial.pdf

18. Mehr, A. D., Nourani, V., Kahya, E., Hrnjica, B., Sattar, A., & Yaseen, Z. (2018). Genetic programming in water resources engineering: A state-of-the-art review. *Journal of Hydrology*. https://doi.org/10.1016/j.jhydrol.2018.09.043

19. Onyelowe, K., Alaneme, G., Igboayaka, C., Orji, F., Ugwuanyi, H., Van Bui, D., & Van Nguyen, M. (2019). Scheffe optimization of swelling, California bearing ratio, compressive strength, and durability potentials of quarry dust stabilized soft clay soil. *Materials Science for Energy Technologies, 2*(1), 67–77. https://doi.org/10.1016/j.mset.2018.10.005

20. Onyelowe, K. C., Ebid, A., Nwobia, L., & Dao-Phuc, L. (2021). Prediction and performance analysis of compression index of multiple-binder treated soil by genetic programming approach. *Nanotechnology for Environmental Engineering*. https://doi.org/10.1007/s41204-021-00123-2

21. Onyelowe, K. C., Iqbal, M., Jalal, F., Onyia, M., & Onuoha, I. (2021). Application of 3 algorithm ANN programming to predict the strength performance of hydrated-lime activated rice husk ash treated soil. *Multiscale and Multidisciplinary Modeling, Experiments and Design.* https://doi.org/10.1007/s41939-021-00093-7

22. Shafabakhsh, G. & Tanakizadeh, A. (2016). Development of asphalt concrete stiffness modulus prediction models using genetic programming. In Conference: 2nd international conference on modern research in civil engineering, architectural & Urban DevelopmentAt: Istanbul-Turkey.

23. Zhang, J. H., Hu, J. K., Peng, J. H., & Zhou, C. (2021). Prediction of resilient modulus for subgrade soils based on ANN approach. *Journal of Central South University, 28*, 898–910. https://doi.org/10.1007/s11771-021-4652-7

24. Coleri, E., & Ahmet, G. (2010). Prediction of subgrade resilient modulus by genetic algorithm and curve shifting methodology as an alternative to nonlinear constitutive models. *Transportation Research Record Journal of the Transportation Research Board., 2170*, 64–73. https://doi.org/10.3141/2170-08

25. Obianyo, I. I., Mahamat, A. A., Anosike-Francis, E. N., Stanislas, T. T., Geng, Y., Onyelowe, K. C., Odusanya, S., Onwualu, A. P., & Soboyejo, A. B. O. (2021). Performance of lateritic soil stabilized with combination of bone and palm bunch ash for sustainable building applications. *Cogent Engineering, 8*(1), 1921673. https://doi.org/10.1080/23311916.2021.1921673

26. Obianyo, I. I., Onwualu, A. P., & Soboyejo, A. B. O. (2020). Mechanical behaviour of lateritic soil stabilized with bone ash and hydrated lime for sustainable building applications. *Case Studies in Construction Materials, 12*(2020), 1–12.

27. Obianyo, I. I., Anosike-francis, E. N., Odochi, G., Geng, Y., Jin, R., Peter, A., & Soboyejo, A. B. O. (2020). Multivariate regression models for predicting the compressive strength of bone ash stabilized lateritic soil for sustainable building. *Construction and Building Materials, 263*, 120677. https://doi.org/10.1016/j.conbuildmat.2020.120677

28. Mahamat, A. A., Boukar, M. M., Ibrahim, N. M., Stanislas, T. T., Bih, N. L., Obianyo, I. I., & Savastano, H. (2021). Machine learning approaches for prediction of the compressive strength of alkali activated termite mound soil. *Applied Sciences, 11*, 4754.

29. BS 1377-2. (1990). Methods of testing soils for civil engineering purposes, British Standard Institute, London.

30. Davidovits, J. (2013). Geopolymer Cement a review. Institut Geopolymer, F-02100 Saint-Quentin, France. [online].

31. American Standard for Testing and Materials (ASTM) C618. (1978). Specification for Pozzolanas. ASTM International, Philadelphia, 1978, USA.

32. American Standard for Testing and Materials (ASTM) E1621-13. (2013). Standard guide for elemental analysis by wavelength dispersion x-ray fluorescence spectrometry, ASTM International, West Conshohocken, PA. https://doi.org/10.1520/E1621-13.

33. BS 1924-2. (2018). Hydraulically bound and stabilized materials for civil engineering purposes-Sample preparation and testing of materials during and after treatment. In British Standard Institute, London.

34. Pallant, J. (2013). SPSS survival manual. McGraw Hill Education, UK.

35. AASHTO. (2004). *Guide for mechanistic-empirical design of new and rehabilitated pavement structures [S]*. AASHTO.

36. Austroads. (2002). Mix design for stabilized pavement materials; Austroads Publication AP-T16, Sydney.

37. El-Bosraty, A. H., Ebid, A. M., & Fayed, A. L. (2020). Estimation of the undrained shear strength of east Port-Said clay using the genetic programming. *Ain Shams Engineering Journal*. https://doi.org/10.1016/j.asej.2020.02.007

38. Ebid, A. M. (2020). 35 Years of (AI) in geotechnical engineering: state of the art. *Geotechnical and Geological Engineering*. https://doi.org/10.1007/s10706-020-01536-7

Dr. Kennedy C. Onyelowe has a PhD in Geotechnical Engineering and he is a senior academic at the MOUA-Umudike, Visiting Fellow at the Kampala International University, Kampala, Uganda, and Visiting Fellow and Proposals External Technical Reviewer at the Research and Innovations Fund, Makerere University, Kampala, Uganda, with multiple teaching and research affiliations in the USA, Australia, India, Egypt, South Africa, Iran, Canada, China, Pakistan, Vietnam, etc. He is currently the Deputy Dean of the College of Eng. & Eng. Technology, MOUAU. He is also the Principal Researcher for Research Group of Geotechnical Engineering, Construction Materials and Sustainability, Hanoi University of Mining and Geology, Hanoi, Vietnam. His research interests are in Geotechnical and Geoenvironmental Engineering. He mentors over 50 young researchers globally. He has over 17 years of industry and research experience and is a registered fellow of various learned academic and professional societies.

Dr. Ahmed M. Ebid Associated Professor, Future University in Egypt, Department of structural Engineering & construction management. He graduated in 1996 from Ain Shams University in Egypt and got his M.Sc. in 2000 in "Reliability analysis in geotechnical engineering" and Ph.D. in 2004 in "Application of genetic programming in geotechnical engineering" both from Ain Shams University. His research areas are FEM model modelling, applying (AI) techniques, design optimization, and reliability analysis.
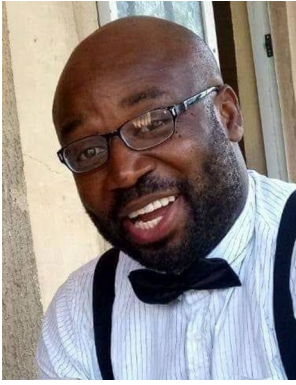
Frank I. Aneke is a Lecturer and an active Researcher at the University of Kwazulu Natal and a registered Professional Geotechnical Engineer with the Institute of Engineering Professionals New Zealand. Dr. Aneke acquired over 15 years of industry and research experience. His research interests span across Geoenvironmental, Pavement Geotechnics, Foundation Engineering as well as unsaturated soil mechanics application in Geotechnical Engineering and sustainable materials development. Dr. Aneke produced several M.Sc. graduates with many others under his supervision.

Nwobia Light Ihenna is a Graduate Assistant at Michael Okpara University of Agriculture, Umudike, Nigeria. He is a passionate interdisciplinary researcher within the field of Engineering, on areas that promote sustainability, particularly in Water and Environmental Engineering, including Geotechnical and Material Engineering, with applications to experimental and soft computing techniques.